Dry Metal Forming Open Access Journal

Fast Manuscript Track

Edited by Frank Vollertsen
Available online at elib.suub.uni-bremen.de

www.drymetalforming.de

Dry Met. Forming OAJ FMT 2 (2016) 072–077
Received 29 April 2016; published 1 June 2016

HPPMS $(Cr_{1-x}Al_x)N+WS_y$ Coatings for the Application in Dry Cold Forging of Steel: Synthesis and Raman Characterization

Kirsten Bobzin[1], Tobias Brögelmann[1], Nathan C. Kruppe[1], Mostafa Arghavani[1], Serhan Bastürk*[1], Fritz Klocke[2], Patrick Mattfeld[2], Daniel Trauth[2], Rafael Hild[2]

[1]Surface Engineering Institute (IOT), RWTH Aachen University, Kackertstr. 15, 52072 Aachen, Germany
[2]Laboratory for Machine Tools and Production Engineering (WZL), RWTH Aachen University, Steinbachstr. 19, 52074 Aachen, Germany

Abstract

Lubricants are applied to reduce friction between workpieces and forming tools in cold forging processes. There is a strong demand to avoid lubricants due to economic, ecological and legislative aspects. PVD coatings took over the tasks of lubricants in numerous applications in the recent years. They may enormously reduce tool and workpiece wear in cold forging or deliver special functions even in the absence of lubricants. However, the abdication of lubricants goes along with the requirement that the dry tribological system has to withstand the increased tribological loads in dry metal cold forging of steel. The combination of $(Cr_{1-x}Al_x)N$ and WS_y within a PVD coating by means of high power pulsed magnetron sputtering (HPPMS) to gain outstanding tribological properties of WS_y with increased abrasive wear resistance of $(Cr_{1-x}Al_x)N$ is a promising candidate in order to replace lubricants on highly loaded tools in dry cold forging. HPPMS technology offers outstanding advantages in terms of dense morphology and high hardness. Using HPPMS-technology, complex-shaped forging tools with surfaces oriented non-parallel to the target can be coated as well. The aim of the current contribution is the investigation of the HPPMS $(Cr_{1-x}Al_x)N+WS_y$ coatings by means of Raman spectroscopy. These coatings were deposited on 1.2379 tool steel using an industrial scale PVD unit. Tribological model tests were conducted using a Pin-on-Disc tribometer (PoD) which simulates dry contacts in cold forging. The analysis of tribological properties included the determination of friction coefficients and wear rates. The contact region was analyzed by Raman spectroscopy after the tribological tests. The investigated $(Cr_{1-x}Al_x)N+WS_y$ coating is a promising candidate to avoid to use of lubricants for the application in dry cold forging process of steel.

Keywords: cold forging, PVD, HPPMS, Raman, CrAlN, WS_2

1 Introduction

Cold forging processes offer advantages such as the maximum degree of material utilization and the associated energy and resource efficiency [1]. In these processes, lubricants and harmful additives are applied to reduce friction between workpieces and forming tools, which are questionable due to ecological, economic, and legislative reasons [2-6]. Physical vapor deposited (PVD) tool coatings are an alternative to lubricants in cold forging processes for an environmentally friendly metal forming. Regarding to this demand, many studies were done previously. Recent studies focus on the avoidance of lubricant usage in metal forming which contributes significantly to waste reduction in manufacturing processes and to the goal of a lubricant-free “green” factory [7].

High power pulsed magnetron sputtering (HPPMS) technology represents an advancement of the dcMS technology. Using this technology, an extremely higher plasma density can be achieved in comparison to conventional dcMS due to high-energy pulses [8]. Coatings deposited by means of HPPMS show outstanding advantages with respect to good mechanical properties, dense morphology and an improved adhesion to the substrate [9]. Furthermore, another positive aspect of the HPPMS technology is the ability to deposit coatings on complex-shaped tools with surfaces oriented non-parallel to the target, which is the case for the cold forging of steel [10].

The ternary system (Cr,Al)N is a promising candidate to withstand extreme tribological loads in the cold forging processes due to its properties such as high

*E-mail address of corresponding author: basturk@iot.rwth-aachen.de

hardness and good abrasion wear resistance, in which high contact pressures up to $\sigma_c = 2{,}500$ MPa are generated [11-13]. Besides, the coating has to reduce friction forces in the same time, which results in a reduced wear rate of the tools. The application of self lubricating coatings is one of the solutions for the reduction of friction forces. Transition metal dichalcogenides (TMD) are widely used as solid lubricants due to their extreme low coefficient of friction (CoF) [14-18]. Among TMDs, molybdenum disulfide (MoS_2) and tungsten disulfide (WS_2) have been the most studied [15,19-23]. Their lubricating character is based on the anisotropic crystal layer structure which consists of e.g. tungsten (W) atom layers located between sulfur (S) atom-arrays. There is a strong covalent bonding between the atoms. However, the layers are loosely bound through comparably weak van der Waals forces. This structure is responsible for the interlamellar mechanical weakness with low shear strength, which results in a macroscopic lubricating effect [24,25]. Application of WS_2 coatings on tools deposited by means of PVD reduces friction but only in vacuum or in inert gas environment [26]. Besides they have a hardness lower than HU = 10 GPa [14]. Therefore, combining the appropriate mechanical properties and wear resistance of (Cr,Al)N with the lubricating effect of WS_2 could promise a suitable solution for replacement of lubricants on highly forced tools in dry cold forging. First studies on WS_2-added HPPMS (Cr,Al)N coatings by means PVD showed satisfying results [19,23]. The main focus of this study was set on studying the HPPMS $(Cr_{1-x}Al_x)N+WS_y$ coatings, characterizing the coating properties and investigating interaction mechanisms after tribological model tests by means of Raman spectroscopy.

2 Experimental procedure

2.1 Deposition process of the $(Cr_{1-x}Al_x)N+WS_y$ coating

Substrates of tool steel 1.2379 (AISI D2, X155CrMoV12) $x_C = 1.540$, $x_{Si} = 0.350$, $x_{Mn} = 0.310$, $x_P = 0.028$, $x_S = 0.008$, $x_{Cr} = 11.520$, $x_{Mo} = 0.730$, $x_V = 0.940$ were employed. All specimens ($\varnothing_{Sample} = 20$ mm, $h_{Sample} = 8$ mm) were hardened and tempered to a hardness of (61.0 ± 0.5) HRC and polished with diamond suspension to an arithmetic mean roughness of Ra ≈ 0.02 µm. Prior to deposition, the specimens were cleaned in a multi-stage ultrasonic bath which contained alkaline solvents. Before the deposition, all specimens were cleaned in an in situ plasma treatment explained in [27]. An industrial coating unit CC800/9 Custom (CemeCon AG, Würselen, Germany) was used. This unit is equipped with two conventional MS cathodes and two HPPMS cathodes. The chemical composition of the deposited coatings were varied using a special target which consists of a $Cr_{0.50}Al_{0.50}$ half and a WS_2 half in form of triangles as explained in [23]. Same experiment setting was used for the production of the samples. A constant mean power of P = 2.5 kW was applied to the cathode in HPPMS mode. A pulse frequency of f = 500 Hz and a pulse length of $t_{on} = 200$ µs were chosen. Further information on the deposition as well as the process parameters can be found in [23]. Figure 1 shows the schematic of the custom target and the sample positions. Contents in the parenthesis give the information on the content of each target sections on the target surface at line of sight in different heights.

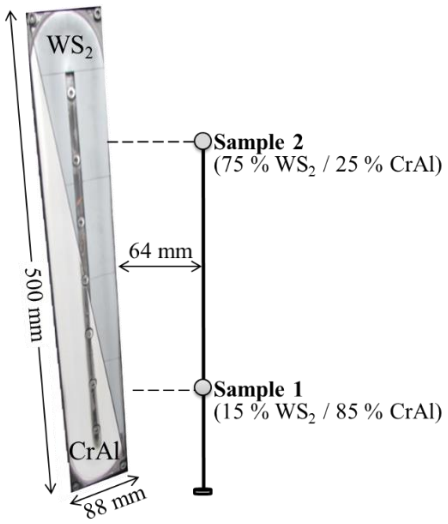

Figure 1: Schematic of the custom target and the sample positions

2.2 Analysis methods

The coating thickness and morphology were analyzed by using scanning electron microscopy (SEM) of type DSM 982 Gemini (Carl Zeiss GmbH, Jena, Germany). The chemical composition of the coatings was determined by using glow discharge optical emission spectroscopy (GDOES) in radio frequency (rf) mode. A GDOES profiler type JY 5000 RF (HORIBA Jobin Yvon Ltd., Kyoto, Japan) equipped with an anode of d = 4 mm was used. The crystallographic phase analysis of the coatings was carried out via X-ray diffractometry (XRD) using grazing incidence (GI) X-ray diffractometer XRD3003 (GE Energy Germany GmbH, Ratingen, Germany). Selected parameters were as follows: GI: ω = 3°; diffraction angle 2θ: 15° to 90°; step width: s = 0.05°; step time: t = 5 s. All measurements were performed using Cu-Kα radiation operated at U = 40 kV and I = 40 mA. A Nano-indenter™ XP (MTS Nano Instruments, Oak Ridge, Tennessee, USA) was applied for the determination of the mechanical properties; universal hardness HU and the modulus of indentation E_{IT}. The penetration depth was kept below 10 % of the top layer thickness. Calculations of the modulus of indentation are based on Oliver and Pharr's equations [28]. A constant Poisson's ratio of υ = 0.25 was assumed. A PoD tribometer (Anton Paar, Ostfildern-Scharnhausen, Germany), was used for the investigation of tribological behavior under dry sliding condition. 1.7131 (AISI 5115, 16MCr5) pins (Ø = 6 mm, Ra = 0.02 µm) were chosen as counterpart. 1.7131 is one of the typical tool materials in cold forging [29]. Pins were pressed in off center position onto the coated specimen with a constant load of

F = 10 N and a radius of r = 2.5 mm at room temperature T = 23 °C and controlled air atmosphere with a relative humidity of RH = 32 (± 2) %. Relative velocity was v = 5 cm/s. Tribological investigations were carried out for a sliding distance of s = 200 m. Wear tracks were first examined by means of confocal laserscanning microscopy (CLSM) with a VK-X210 microscope (Keyence GmbH, Neu-Isenburg, Germany). Besides they were also examined using a confocal Raman spectrometer inVia REFLEX (RENISHAW, Gloucestershire, United Kingdom). A laser with excitation wavelength λ = 532 nm with a 50 % laser intensity during t = 10 s of exposure time was used. The Raman spectra ϑ = 200 – 2,000 cm^{-1} were acquired from the center of the wear tracks. Figure 2 shows the used micro-Raman spectrometer at IOT.

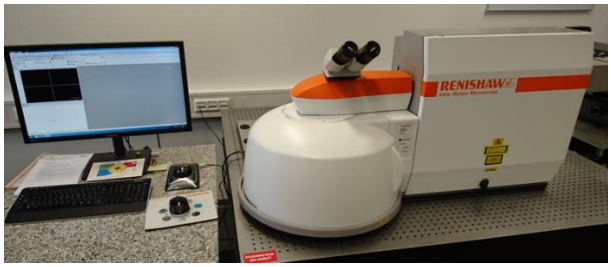

Figure 2: Confocal micro-Raman spectrometer at IOT

3 Results and discussion

3.1 Coating properties

Cross section fractures of the two HPPMS $(Cr_{1-x}Al_x)N+WS_y$ coatings are shown in Figure 3. The thicknesses of the coatings are as follows: $d_{Sample1}$ = 3.85 µm and $d_{Sample2}$ = 4.58 µm. Both coatings show a crystalline microstructure.

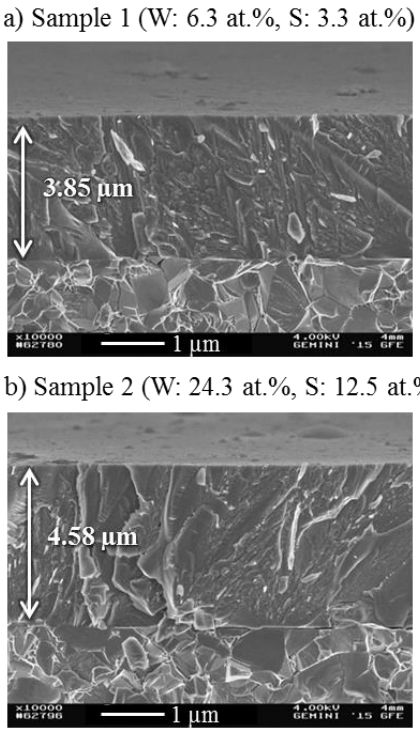

Figure 3: SEM cross section fractures of the $(Cr_{1-x}Al_x)N+WS_y$ coatings: a) sample 1 and b) sample 2

Table 1 shows the chemical composition of the deposited coatings as measured by GDOES. Al content drops from x_{Al} = 41.5 at.% in sample 1 to x_{Al} = 24.1 at.% in sample 2 due to the experimental setting. For the WS_y, y means the ratio of number of atoms N_S/N_W and corresponds to about 0.5 in both samples. This means that the coatings are S-poor. Therefore, a sub-stoichiometric composition of WS_2 is expected.

Table 1: Chemical composition of the $(Cr_{1-x}Al_x)N+WS_y$ coatings as determined by GDOES

Element [at.%]	Sample 1	Sample 2
Al	41.5	24.1
Cr	31.7	24.2
N	17.3	15.0
S	3.3	12.5
W	6.3	24.3

For further investigations, the phase composition of the HPPMS $(Cr_{1-x}Al_x)N+WS_y$ coatings was analyzed using XRD. Figure 4 shows the XRD patterns. Both coatings present a crystal structure. Patterns indicate that the crystalline structure of the $(Cr_{1-x}Al_x)N$ phase is predominantly cubic. No peaks of the different phases of WS_2 are detectable.

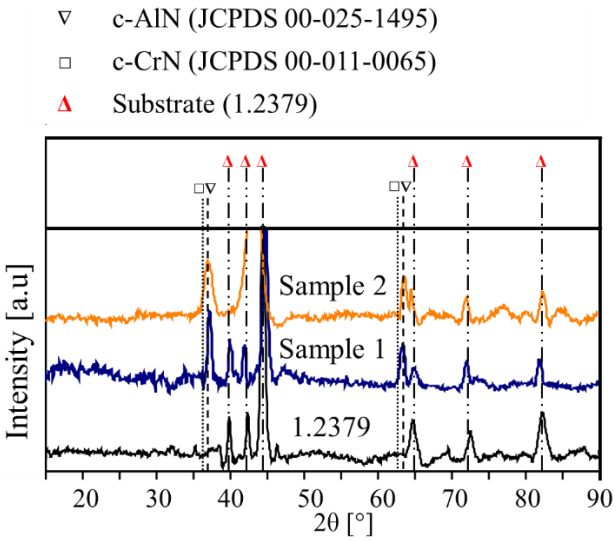

Figure 4: XRD patterns of the HPPMS $(Cr_{1-x}Al_x)N+WS_y$ coatings as well as uncoated 1.2379 substrate

Deposited coatings do not differ in mechanical properties largely. Sample 1 shows a bit higher mechanical properties: $HU_{Sample1}$ = (16.4 ± 1.5) GPa and $E_{IT,\ Sample1}$ = (157.6 ± 22.8) GPa, whereas sample 2 has the following values $HU_{Sample2}$ = (14.1 ± 1.1) GPa and $E_{IT,\ Sample2}$ = (145.0 ± 17.3) GPa.

3.2 System properties

The friction behavior of the deposited coatings was investigated by model tests in PoD tribometer under dry sliding conditions. Figure 5 shows the CoF of the

coatings as well as the uncoated substrate 1.2379 as reference against 1.7131 counterpart pin.

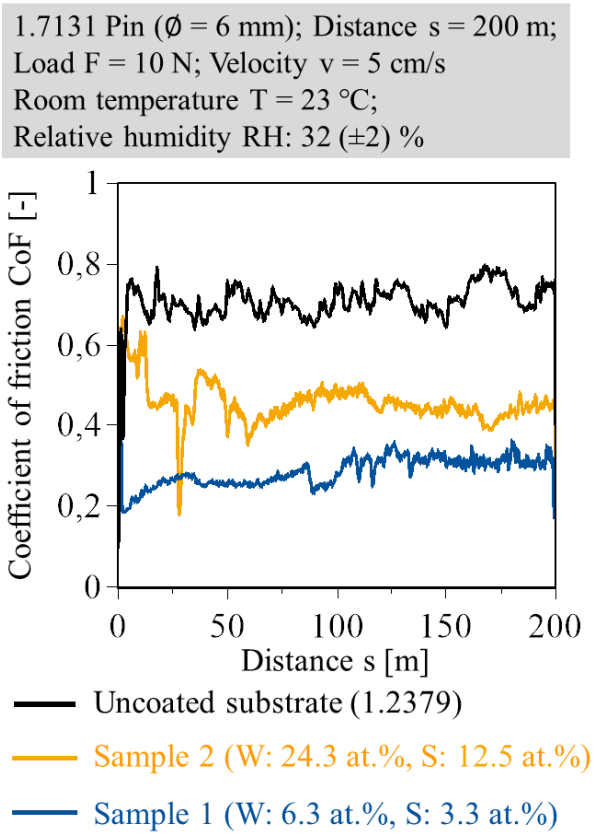

Figure 5: Coefficient of friction of the $(Cr_{1-x}Al_x)N+WS_y$ coated samples and uncoated substrate using PoD tribometer

Investigations have shown that both coated samples exhibit lower CoF compared to the uncoated substrate, whereas the coating sample 1 exhibits the lowest CoF $\mu_{Sample\ 1} = 0.25$. Sample 2 has a CoF of $\mu_{Sample\ 2} = 0.4$. For further investigation, the wear rate w was calculated using the wear volumes of the 1.7131 counterparts as well as of the HPPMS $(Cr_{1-x}Al_x)N+WS_y$ coated samples after tribological model tests by PoD tribometer measured by means of CLSM. Tribological model test with sample 1 indicates the lowest wear rate for the used counterpart $w_{Pin,Sample\ 1} = 4.1 \cdot 10^3\ \mu m^3/Nm$ and on the sample's surface $w_{Sample\ 1} = 0.9 \cdot 10^3\ \mu m^3/Nm$. Wear rate for the used counterpart and on the sample's surface is considerably higher showing $w_{Pin,Sample\ 2} = 25.2 \cdot 10^3\ \mu m^3/Nm$ and $w_{Sample\ 2} = 15.5 \cdot 10^3\ \mu m^3/Nm$ respectively. It is not possible to explain these phenomena only in support of mechanical properties. This difference is based on the quite differing CoFs.

The investigation of the worn track by Raman spectroscopy was used to understand the chemical phenomena occurring at the contact area responsible of the observed friction behavior. It is very helpful to elucidate the friction mechanisms. This way, the chemical bondings, phase composition and the wear products can be defined [31-33]. Coated samples and the 1.7131 counterpart were investigated after PoD model tests, since the formation of self-lubricating sulphides is another aspect causing a reduction of the friction. For this purpose, the tip of the counterpart and areas in the wear track on the coating after PoD model tests were investigated along with a spectrum from the as deposited coating for reference. Figure 6 shows the Raman spectra of all these three different measurements on both samples.

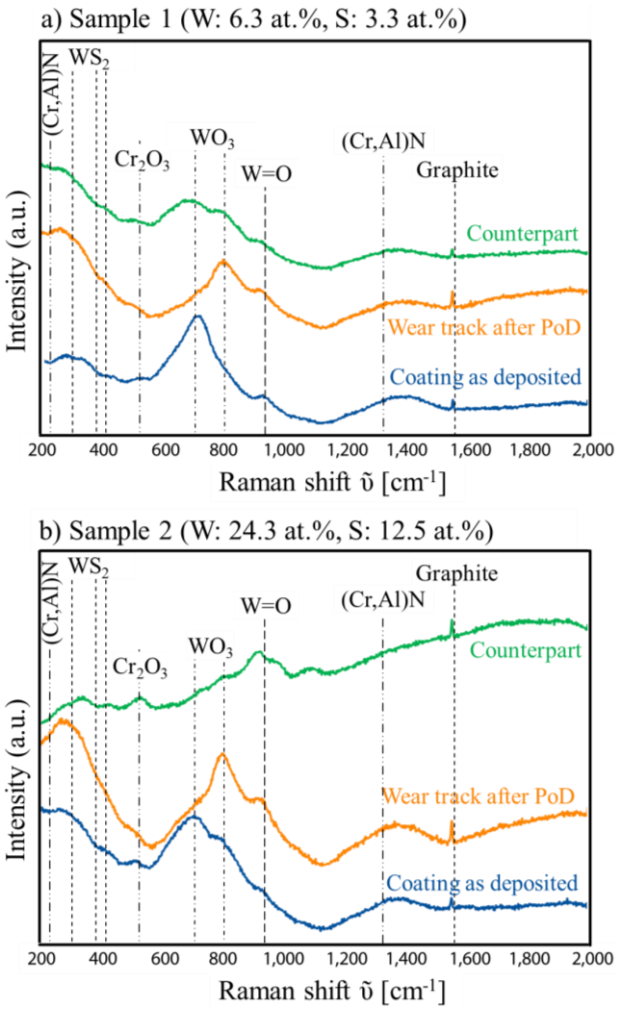

Figure 6: Raman spectra of the HPPMS $(Cr_{1-x}Al_x)N+WS_y$ coated samples as deposited and after PoD model tests as well as counterpart

Raman spectra of the both unworn coatings in as deposited conditions seem to be similar. It is observed that the WO_3 bonding centered at $\tilde{\upsilon} = 807\ cm^{-1}$ is not emerged for sample 1. On the worn tracks this peak becomes detectable for both coatings. Indeed, for sample 1, the WO_3 peak centered at $\tilde{\upsilon} = 710\ cm^{-1}$ transforms completely to $\tilde{\upsilon} = 807\ cm^{-1}$, whereas it was not detectable in as deposited condition at all. The origin of the peaks at $\tilde{\upsilon} = 960\ cm^{-1}$ is attributed to the formation of nanocrystalline oxides with Mo=O bonds [30]. Graphite is also detected at $\tilde{\upsilon} = 1{,}580\ cm^{-1}$. Carbon most likely originates from surface contaminations of the coating. Sliding in air atmosphere with a humidity of RH = 32 (±2) % leads to the reaction of the TMD-based coating with water vapor. This reaction results in oxidation and the incorporation of contaminants [16]. This Raman study has shown that the material in the wear tracks is formed mainly by a mixture of W oxides with different stoichiometries and (Cr,Al)N. A

formation of self-lubricating sulphides could not be proven on the wear tracks with the help of these Raman investigations. Increasing laser intensity in Raman investigating did not result in the observation of such tribo-chemical reaction products neither. One reason could be the short distance in the model tests. Furthermore, the spectra of the counterparts show several differences. The counterpart of sample 2 exhibits a clear peak of Cr_2O_3 centered at $\tilde{\upsilon} = 501\ cm^{-1}$, whereas sample 1 shows almost none. Besides, nanocrystalline oxides with Mo=O bonds is very strong for the counterpart of sample 2. Bouleva et al. have shown that the peak intensity becomes stronger with a decreasing grain size [34]. It can be assumed that the formation of the WO_3 and Cr_2O_3 bonds on the counterpart is responsible for the tribological behavior of the sample 2. Muratore et al. reported in situ Raman investigations in their studies where they observed a transformation from MoS_2 to MoO_3 together with an increase in CoF which was associated with buildup of the abrasive oxide compound [35].

4 Conclusion and outlook

In this study two HPPMS $(Cr_{1-x}Al_x)N+WS_y$ coatings with different W- and S-contents were deposited on tool steel 1.2379. After characterization of the coating properties, samples were investigated regarding their tribological behavior. For this purpose, application oriented wear tests on two samples with different chemical compositions were conducted along with an uncoated substrate for reference using a PoD tribometer. Sample 1 $x_W = 6.3$ at.%, $x_S = 3.3$ at.% showed better tribological properties. Raman investigations have shown that this phenomenon is possibly due to the less formation of WO_3 and Cr_2O_3 bonds on the counterpart which assumed to be responsible for a higher CoF. $(Cr_{1-x}Al_x)N$ coatings in combination with self-lubricating WS_y deposited using HPPMS technology offers a high potential for lubricant-free "green" cold forging of steel.

Acknowledgements

The research was funded by the German Research Foundation (Deutsche Forschungsgemeinschaft DFG) within the priority program „Dry metal forming – sustainable production through dry processing in metal forming (Trockenumformen – Nachhaltige Produktion durch Trockenbearbeitung in der Umformtechnik (SPP 1676).

References

[1] F. Klocke: Manufacturing processes 4 - Forming, Springer, (2013).

[2] H. Czichos, K.-H. Habig, Tribologie-Handbuch: Tribometrie, Tribomaterialien, Tribotechnik, 3., Aufl. ed. ed., Vieweg+Teubner Verlag / GWV Fachverlage GmbH Wiesbaden, Wiesbaden (2010).

[3] F. Klocke, T. Maßmann, K. Bobzin, E. Lugscheider, N. Bagcivan, Carbon based tool coatings as an approach for environmentally friendly metal forming processes, Wear 260 (2006) 287–295.

[4] F. Klocke, T. Maßmann, K. Gerschwiler, Combination of PVD tool coatings and biodegradable lubricants in metal forming and machining, Wear 259 (2005) 1197–1206.

[5] K. Bobzin, N. Bagcivan, P. Immich, C. Warnke, F. Klocke, C. Zeppenfeld, P. Mattfeld, dvancement of a nanolaminated TiHfN/CrN PVD tool coating by a nano-structured CrN top layer in interaction with a biodegradable lubricant for green metal forming, Surface and Coatings Technology 203 (2009) 3184–3188.

[6] E. Lugscheider, K. Bobzin, C. Piñero, F. Klocke, T. Massmann, Development of a superlattice (Ti,Hf,Cr)N coating for cold metal forming applications, Surface and Coatings Technology 177-178 (2004) 616–622.

[7] F. Vollertsen, F. Schmidt: Dry Metal Forming: Definition, Chances and Challenges. Int. J. Precision Engineering and Manufacturing – Green Technology 1/1 (2014) 59–62.

[8] J. Alami, P.A.O. Persson, D. Music, J.T. Gudmundsson, J. Böhlmark, U. Helmersson, Ion-assisted physical vapor deposition for enhanced film properties on nonflat surfaces, Journal of Vacuum Science and Technology A: Vacuum, Surfaces and Films 23-2 (2005) 278.

[9] K. Bobzin, N. Bagcivan, P. Immich, S. Bolz, R. Cremer, T. Leyendecker, Mechanical properties and oxidation behaviour of (Al,Cr)N and (Al,Cr,Si)N coatings for cutting tools deposited by HPPMS, Thin Solid Films 517-3 (2008) 1251.

[10] N. Bagcivan, K. Bobzin, S. Theiß, $(Cr_{1-x}Al_x)N$: A comparison of direct current, middle frequency pulsed and high power pulsed magnetron sputtering for injection molding components, Thin Solid Films 528 (2013) 180-186.

[11] N. Bay, A. Azushima, P. Groche, I. Ishibashi, M. Merklein, M. Morishita, T. Nakamura, S. Schmid, M. Yoshida, Environmentally benign tribo-systems for metal forming, CIRP Annals - Manufacturing Technology 59 (2010) 760–780.

[12] J. Lin, B. Mishra, J.J. Moore, W.D. Sproul, Microstructure, mechanical and tribological properties of $Cr_{1-x}Al_xN$ films deposited by pulsed-closed field unbalanced magnetron sputtering (P-CFUBMS), Surface and Coatings Technology 201 (2006) 4329–4334.

[13] N. Bagcivan, K. Bobzin, R.H. Brugnara, Investigation of the properties of low temperature $(Cr_{1-x}Al_x)N$ coatings deposited via hybrid PVD DC-MSIP/HPPMS, Mat.-wiss. u. Werkstofftech. 44 (2013) 667–672.

[14] T. Mang (Ed.), Lubricants and lubrication, 2., completely rev. and extended ed. ed., Wiley-VCH, Weinheim (2007).

[15] C. Donnet, A. Erdemir, Solid lubricant coatings: recent developments and future trends, Tribology Letters 17 (2004) 389–397.

[16] P. Mutafov, M. Evaristo, A. Cavaleiro, T. Polcar, Structure, mechanical and tribological properties of self-lubricant W–S–N coatings, Surface and Coatings Technology 261 (2015) 7–14.

[17] C. Donnet, J.M. Martin, T. Le Mogne, M. Belin, Super-low friction of MoS_2 coatings in various environments, Tribology International 29 (1996) 123–128.

[18] A. Aubert, J. Nabot, J. Ernoult, P. Renaux, Preparation and properties of MoS_x films grown by d.c. magnetron sputtering, Surface and Coatings Technology 41 (1990) 127–134.

[19] K. Bobzin, T. Brögelmann, N. Kruppe, S. Bastürk, F. Klocke, P. Mattfeld, D. Trauth, Tribological Behavior of $(Cr_{1-x}Al_x)N/WS_y$ PVD Tool Coatings for the Application in Dry Cold Forging of Steel, Dry Metal Forming Open Access Journal 1 (2015) 152–158.

[20] F. Klocke, D. Trauth, P. Mattfeld, A. Shirobokov, K. Bobzin, T. Brögelmann, S. Bastürk, Multiscale FE-Studies of Contact Stresses of Dry and Lubricated Shot Peened Workpiece Surfaces, Dry Metal Forming Open Access Journal 1 (2015) 11–16.

[21] F. Klocke, D. Trauth, R. Hild, P. Mattfeld, K. Bobzin, S. Bastürk, T. Brögelmann, Numerical Analysis of the Tribological Mode of Action in Cold Forming of Sinus Waved Surfaces Structures, Dry Metal Forming Open Access Journal 1 (2015) 137-142.

[22] K. Bobzin, T. Brögelmann, S. Bastürk, F. Klocke, P. Mattfeld, D. Trauth, P. Polcik, S. Kolozsvari, Influence of the Composition on the Properties of $(Cr_{1-x}Al_x)N/Mo_yS_z$ PVD

Coatings, Advanced Engineering Materials, DOI: 10.1002/adem.201500499.
[23] K. Bobzin, T. Brögelmann, R. H. Brugnara, N. C. Kruppe, S. Bastürk, F. Klocke, P. Mattfeld, R. Hild, D. Trauth, Influence of the Chemical Composition on the Properties of HPPMS $(Cr_{1-x},Al_x)N/WS_y$ Coatings for the Application on Dry Cold Forging Processes, 12th International Conference THe "A" Coatings 2016, Hannover, Germany (2016).
[24] K. Bobzin, E. Lugscheider, R. Nickel, N. Bagcivan, A. Krämer, Wear behavior of $Cr_{1-x}Al_xN$ PVD-coatings in dry running conditions, Wear 263 (2007) 1274–1280.
[25] J.-F. Yang, B. Parakash, J. Hardell, Q.-F. Fang, Tribological properties of transition metal di-chalcogenide based lubricant coatings, Front. Mater. Sci. 6 (2012) 116–127.
[26] B. Deepthi, Harish C. Barshilia, K.S. Rajam, Manohar S. Konchady, Devdas M. Pai, Jagannathan Sankar, Alexander V. Kvit, Structure, morphology and chemical composition of sputter deposited nanostructured Cr–WS_2 solid lubricant coatings, Surface and Coatings Technology 205-2 (2010) 565-574.
[27] K. Bobzin, T. Brögelmann, S. Basturk, F. Klocke, P. Mattfeld, D. Trauth, Development of an in situ Plasma Treatment of X155CrMoV12 for a (Cr,Al)N PVD Tool Coating for Dry Metal Forming in Cold Forging, Dry Metal Forming Open Access Journal, 1 (2015) 57-62.
[28] W.C. Oliver, G.M. Pharr, An improved technique for determining hardness and elastic modulus using load and displacement sensing indentation experiments, Journal of Materials Research 7 (1992) 1564–1583.
[29] K.-H. Grote, E.K. Antonsson, Springer handbook of mechanical engineering, Springer, Berlin (2009).
[30] A. Baserga, V. Russo, F. Di Fonzo, A. Bailini, D. Cattaneo, C.S. Casari, A. Li Bassi, C.E. Bottani, Nanostructured tungsten oxide with controlled properties: Synthesis and Raman characterization, Thin Solid Films 515 (2007) 6465–6469.
[31] J.C. Sánchez-López, D. Martínez-Martínez, C. López-Cartes, A. Fernández, Tribological behaviour of titanium carbide amorphous carbon nanocomposite coatings: From macro to the micro-scale, Surface and Coatings Technology 202 (2008) 4011-4018.
[32] J.C. Sánchez-López, D. Martínez-Martínez, M.D. Abad, A. Fernández, Metal carbide/amorphous C-based nanocomposite coatings for tribological applications, Surface and Coatings Technology 204 (2009) 947-954.
[33] S. El Mrabet, M.D. Abad, J.C. Sánchez-López, Identification of the wear mechanism on WC/C nanostructured coatings, Surface and Coatings Technology 206 (2011) 1913–1920.
[34] M. Boulova, G. Lucazeau, Crystallite Nanosize Effect on the Structural Transitions of WO_3 Studied by Raman Spectroscopy, Journal of Solid State Chemistry 167 (2002) 425-434.
[35] C. Muratore, J. E. Bultman, S. M. Aouadi, A. A. Voevodin, In situ Raman spectroscopy for examination of high temperature tribological processes, Wear 270 (2011) 140-145.